Wiley
International Journal of Antennas and Propagation
Volume 2025, Article ID 5532772, 13 pages
https://doi.org/10.1155/ijap/5532772

WILEY

Research Article

A Bi-Cylindrical Lens for a DRGH Antenna

Pieter Roodt, Johann Wilhelm Odendaal, Johan Joubert, and Bennie Jacobs

Department of Electrical, Electronic and Computer Engineering, University of Pretoria, Pretoria 0002, South Africa

Correspondence should be addressed to Johann Wilhelm Odendaal; wimpie@up.ac.za

Received 16 January 2025; Revised 25 July 2025; Accepted 28 July 2025

Academic Editor: Rajashik Paul

Broadband double-ridged guide horn (DRGH) antennas are extensively used in antenna measurement and electromagnetic compatibility and interference testing, especially the 1–18 GHz DRGH antenna, which is widely accepted as a standard for this band. Increasing the gain of the DRGH will result in higher field strengths for EMI testing and increased sensitivity in antenna testing facilities. In this paper, a complete wideband near-field *E*- and *H*-plane phase center analysis is performed with CST, at observation points over a region inside the flared section and also outside the aperture of the DRGH. A new plano-convex intersecting bi-cylindrical lens was designed using the two discrete phase centers corresponding to the statistical mode of samples from the population of phase centers obtained from the simulated phase distributions. This new lens is a practical implementation with both convex surfaces on the inside and a planar surface on the outside of the DRGH. This makes manufacturing and mounting the lens much easier without significantly increasing the size of the DRGH antenna. The bi-cylindrical lens significantly increases the boresight gain of the DRGH antenna, while simultaneously reducing the variation in 3 dB beamwidth over most of the operating band.

1. Introduction

Double-ridged guide horn (DRGH) antennas are widely used in antenna and electromagnetic compatibility/interference (EMC/I) testing facilities as feed antennas and gain transfer standards. MIL-STD-461G specify the dimensions of the 1–18 GHz DRGH antenna to be used for EMI and EMC testing purposes with the device under test remaining within the 3 dB beamwidth of the DRGH [1]. To comply with the high field strengths required for EMI testing and to increase sensitivity in antenna testing facilities, a DRGH antenna with high gain values and constant 3 dB beamwidths over frequency will be an advantage.

Employing extensive numerical simulation, a number of studies aimed to optimize and improve the VSWR and suppression of higher-order modes to eliminate pattern deterioration (breakup) of wideband DRGH antennas [2–7]. Recently, some studies focused on improving the *E*-plane aperture efficiency of the DRGH antenna to improve the gain and beamwidth performance. In [8, 9], a rectangular dielectric slab and a significantly larger spherical dielectric structure between the ridges were used to increase the gain of a DRGH. Trial and error followed by numerical optimization was used to design the dielectric structures. A single cylindrical plano-convex lens was used to improve the phase efficiency in the *E*-plane of a DRGH [10]. The lens was designed using a spherical approximation for the phase distribution in the *E*-plane of the DRGH. Employing numerical optimization, a modified axial symmetric plano-convex off-body dielectric lens to increase the gain for automotive immunity testing is presented in [11]. The *E*- and *H*-plane sides of the lens were removed to different degrees to obtain a small off-body lens. In [12], a small, truncated Luneburg lens is used between the ridges to increase the gain of the DRGH. A small axial symmetric hyperbolic lens between the ridges is used to increase the gain of a DRGH in [13]. The lens is designed using an approximation for the *E*-plane path length difference between the edge of the flare and the axial distance of the antenna.

The aperture phase distribution of a DRGH differs significantly in the *E*- and *H*-plane due to the ridges in the flared section. In [14], an off-body plano-convex cylindrical

lens for the E-plane and a cylindrical lens for the H-plane were used in front of a conventional DRGH to increase the gain. The lens was designed using a probe to measure the aperture phase variation in the E- and H-plane at the highest operating frequency. In [15], tapered ridge profiles were introduced to increase the low-frequency gain of the DRGH and achieve more constant 3 dB beamwidths over the operating frequency band. The width of the ridges was tapered along the axial length of the DRGH to increase the effective radiating aperture and improve the H-plane phase efficiency.

In this paper, the radiation properties of the modified DRGH from [15] are further improved with the design of a plano-convex intersecting bi-cylindrical lens inside the flared section of the DRGH without significantly increasing the overall dimensions of the antenna. The bi-cylindrical lens significantly increases the boresight gain of the DRGH antenna, while simultaneously reducing the variation in 3 dB beamwidth over most of the operating band. An accurate numerical CST [16] model was developed, and the E- and H-plane phase centers for this modified DRGH antenna were determined by analyzing the phase distributions over the entire frequency range, axial region inside the flared section, and also outside the aperture of the DRGH. Employing statistical analysis on this frequency and spatial phase distributions, three sets of possible E- and H-plane phase centers were estimated as the mode, 1st quartile, and 3rd quartile. The directivity performance was investigated using lenses designed with these three sets of phase centers to find the most suitable estimate for the E- and H-plane phase centers. The performance of this plano-convex bi-cylindrical lens was compared to two conventional hyperbolic profile lenses, implemented in a plano-convex axial symmetric structure, and designed using the E- and H-plane phase centers, respectively. The proposed intersecting bi-cylindrical lens achieved a directivity of approximately 2 dB higher than the two axial symmetrical lenses, over the operating frequency band of the modified DRGH antenna. The bi-cylindrical lens increased the maximum boresight gain of the modified DRGH antenna by approximately 7 dB and simultaneously reduced the variation in 3 dB beamwidth from $\pm 10^{\circ}$ for the modified DRGH to less than $\pm 5^{\circ}$ over the frequency range from 4 to 18 GHz in both the E- and H-plane.

The design and performance of the plano-convex intersecting bi-cylindrical lens are presented in Section 2. Section 3 presents the measured and simulated results for the DRGH, with concluding remarks in Section 4.

2. Wideband Bi-Cylindrical Lens Design

2.1. E- and H-Plane Phase Centers. The phase center of an antenna is a crucial design parameter used in the design of antenna systems that include reflectors and lenses. The analysis and determination of the phase center of the DRGH antenna are more difficult due to the large operating bandwidth of the antenna and the dielectric lens being placed in the near-field. The modified DRGH antenna [15] was used as a baseline reference antenna. All dimensions and design optimization of the ridge profiles for the modified DRGH antenna are described in [15] and summarized in Table 1. Using the dimensions from [15], an accurate numerical CST model was developed for the modified DRGH antenna (Figure 1(a)), and the E- and H-plane phase centers for this modified DRGH antenna were determined by analyzing the CST simulated field distributions over the entire frequency range and axial region inside the flared section and outside the aperture of the DRGH (Figure 1(b)).

Table 1: Dimensions of the modified DRGH [15].

Description	Dimension (mm)
Aperture width (A)	242
Aperture height (B)	136
Axial length (C)	209.8
Ridge width at feed	9.6
Ridge width for linear taper at aperture	70.43

The positions of the phase center for each frequency and observation point are estimated by minimizing the difference between the simulated phase distribution and the spherical phase front from the estimated phase center position. Figures 2 and 3 show the simulated phase distributions and the spherical phase fronts calculated from the estimated phase center positions for a number of discrete frequencies and observation points in the E- and H-plane of the DRGH antenna, respectively.

To limit the size of the final antenna, an in-flare lens was designed. The phase centers for the bi-cylindrical lens were estimated using the simulated field distributions over the entire frequency range and axial region inside the flared section of the DRGH, occupied by the proposed lens, for the E- and H-plane, respectively (Figure 4).

Figure 5 shows a histogram of the E-plane phase center offset, relative to the origin in Figure 1, using simulated data every 1 GHz from 1 to 18 GHz over a region, $r_1 = 110$ mm to $r_2 = 180$ mm, coinciding with the position of the bi-cylindrical lens inside the aperture of the DRGH. Employing statistical analysis on this frequency and spatial phase distributions, a set of three possible phase centers was estimated for the E- and H-plane (these are the modes, 1st quartile and 3rd quartile of the dataset). The offset of the phase center corresponding to the mode in the E-plane of the DRGH for all frequencies and observation positions, indicated by the red line in the box plot above the graph, results in a phase center position, $z = 61.29$ mm. The red bar in the box plot above the graph represents the phase center offsets between the 1st quartile (−73.91 mm) and 3rd quartile (−55.95 mm), respectively. Figure 6 shows a histogram of the H-plane phase center offset, relative to the origin in Figure 1, using simulated data every 1 GHz from 1 to 18 GHz over a region, $r_1 = 110$ mm to $r_2 = 205$ mm. The offset of the phase center corresponding to the mode in the H-plane of the DRGH for all frequencies and observation positions corresponds to a phase center position $z = -3.17$ mm, and the phase center offsets using the 1st quartile (−4.54 mm) and 3rd quartile (23.64 mm), respectively.

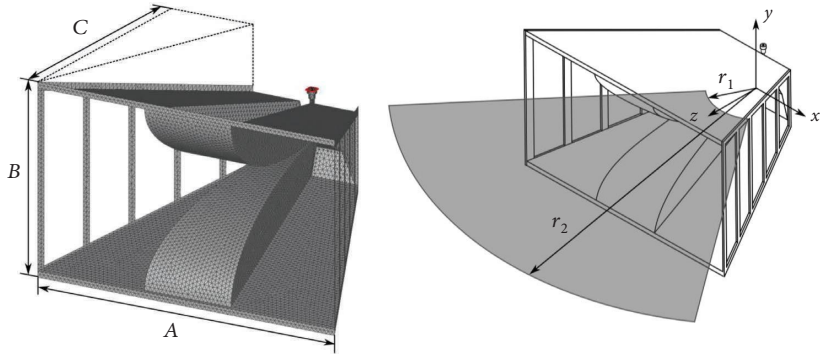

FIGURE 1: (a) CST model of the modified DRGH antenna [15] and (b) the region of observation points for estimating the H-plane phase distribution of the DRGH antenna.

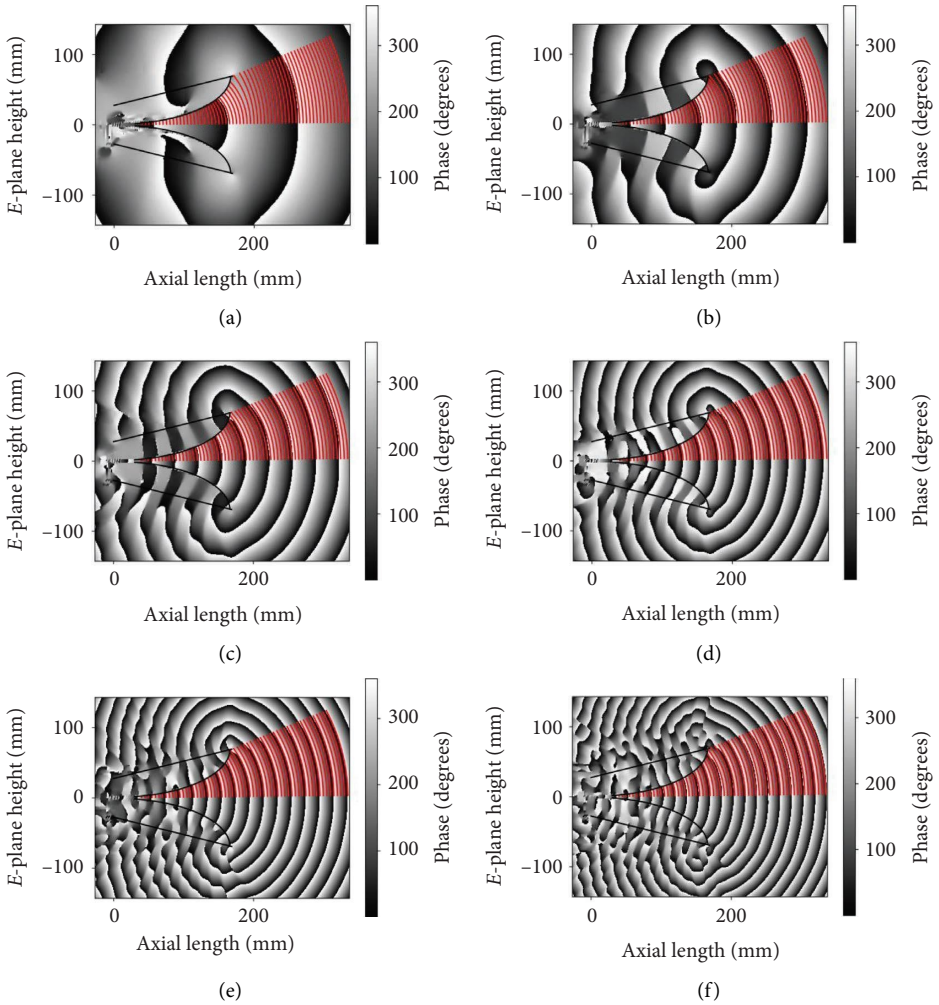

FIGURE 2: Simulated phase distributions and spherical phase fronts calculated from the estimated phase center positions at (a) 3 GHz, (b) 6 GHz, (c) 9 GHz, (d) 12 GHz, (e) 15 GHz, and (f) 18 GHz for the E-plane of the DRGH.

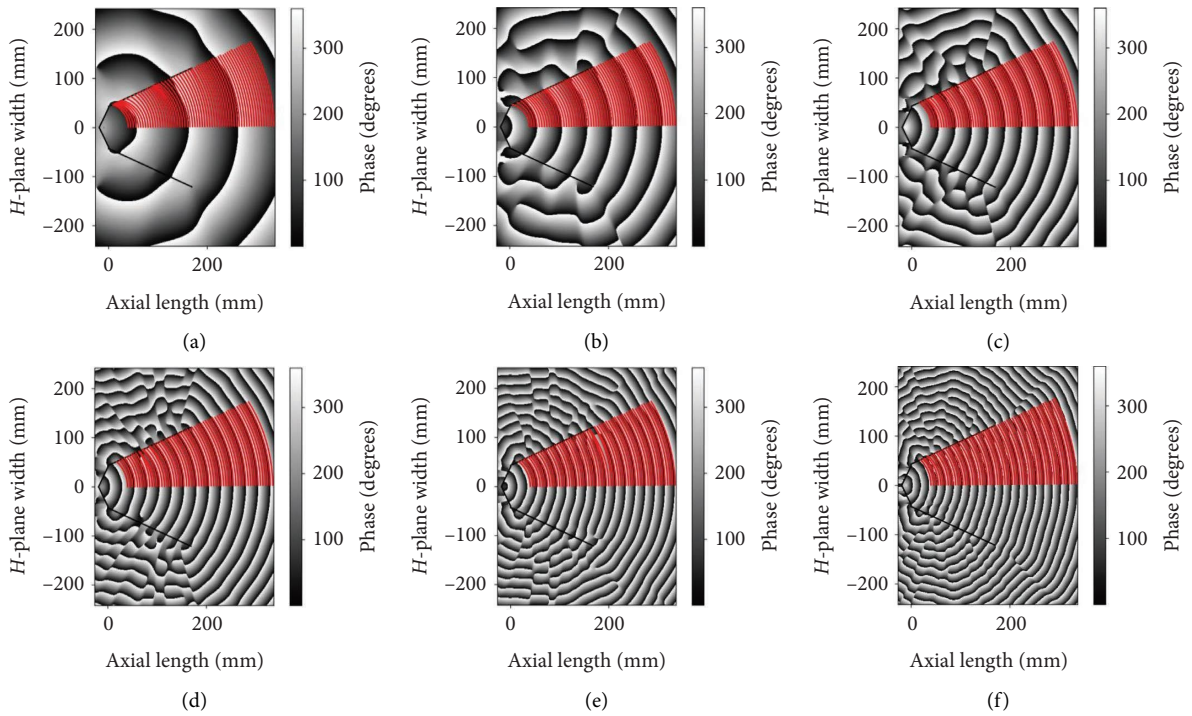

Figure 3: Simulated phase distributions and spherical phase fronts calculated from the estimated phase center positions at (a) 3 GHz, (b) 6 GHz, (c) 9 GHz, (d) 12 GHz, (e) 15 GHz, and (f) 18 GHz for the H-plane of the DRGH.

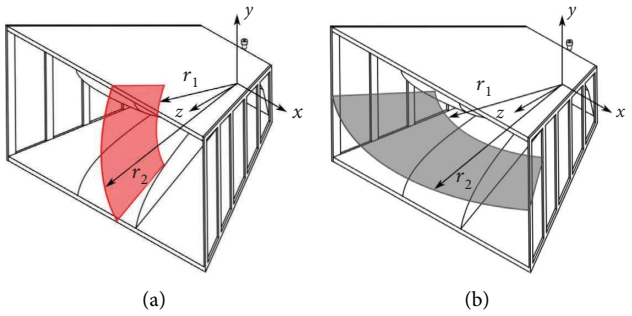

Figure 4: The region of observation points considered for estimating the E- and H-plane phase centers of the DRGH antenna. (a) E-plane. (b) H-plane.

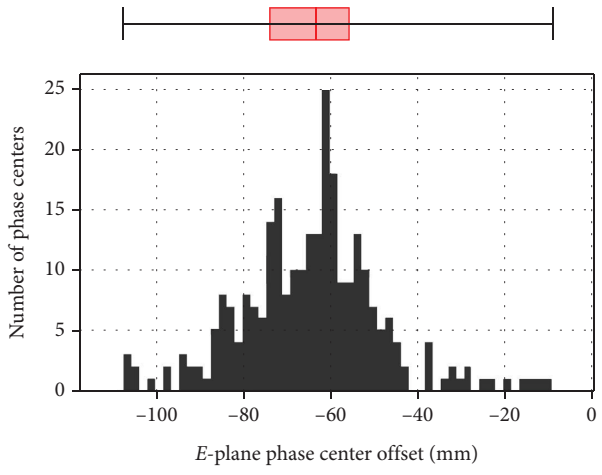

Figure 5: Histogram of the E-plane phase center offset, relative to the origin, using simulated data every 1 GHz from 1 to 18 GHz over a region, r_1 = 110 mm to r_2 = 180 mm.

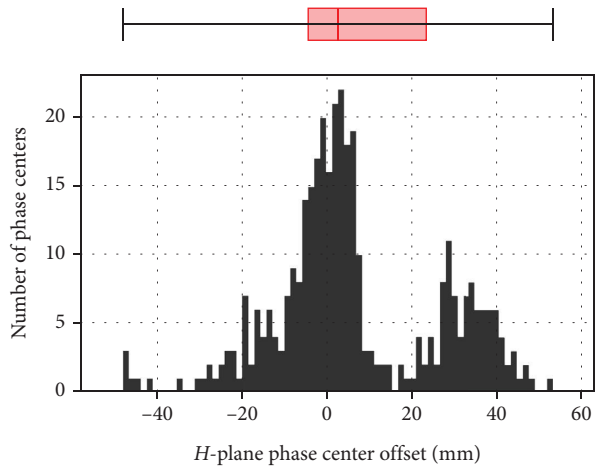

Figure 6: Histogram of the H-plane phase center offset, relative to the origin, using simulated data every 1 GHz from 1 to 18 GHz over a region, $r_1 = 110$ mm to $r_2 = 205$ mm.

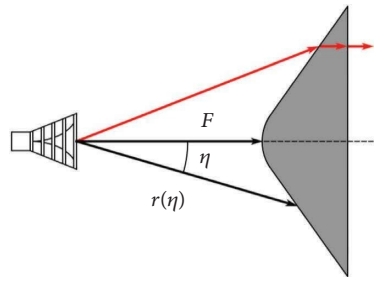

Figure 7: Design of a single refracting surface, hyperbolic lens profile.

Table 2: Dimensions of the axial symmetric lenses.

		***E*-plane**		
Symbol	**Quartile 1 (mm)**	**Mode (mm)**	**Quartile 3 (mm)**	**Description**
P_E	−73.91	−61.29	−55.95	Phase center offset from origin
R_E	94.89	107.51	112.85	Distance, phase center to aperture
F_E	67.36	82.89	89.29	E-plane focal length
D_E	100	100	100	Lens diameter
		***H* -plane**		
Symbol	**Quartile 1 (mm)**	**Mode (mm)**	**Quartile 3 (mm)**	**Description**
P_H	−4.54	3.17	23.64	Phase center offset from origin
R_H	164.26	171.97	192.44	Distance, phase center to aperture
F_H	147.69	155.46	178.21	H-plane focal length
D_H	100	100	100	Lens diameter

2.2. The Bi-Cylindrical Lens. The effect of the variation in estimated phase center positions on the directivity performance of the antenna was investigated using an axial symmetric hyperbolic profile dielectric lens as shown in Figure 7. The hyperbolic lens profile is described by

$$r(\eta) = \frac{(n-1)F}{n\cos(\eta) - 1}, \quad (1)$$

with

$$n = \sqrt{\mu_r \epsilon_r}, \quad (2)$$

where F is the focal distance, n is the refractive index of the dielectric medium, ϵ_r is the relative permittivity, and μ_r is the relative permeability of the dielectric medium.

Different hyperbolic profile lenses were implemented in Teflon using the phase center values corresponding to the 1st quartile, 3rd quartile, and the mode of the dataset, for the E- and H-plane phase centers, respectively. A diameter of 100 mm was used to obtain a large lens aperture size and still have a lens thickness that would fit within the horn, without intersecting with the ridges. Table 2 gives the dimensions for the axial symmetric dielectric lenses using

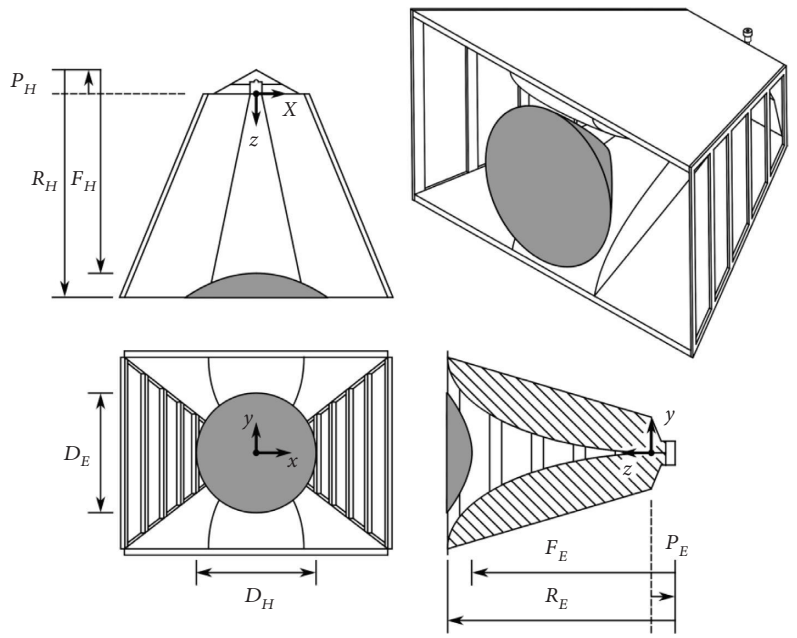

Figure 8: The DRGH antenna with an axial symmetric dielectric lens to investigate the effect of different phase centers on the directivity performance of the antenna.

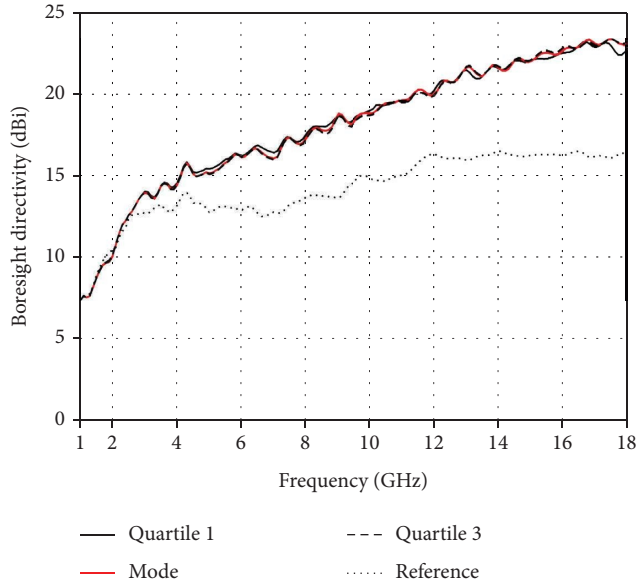

Figure 9: Boresight directivities of the DRGH antenna with an axial symmetric lens and three different E-plane focal distances, compared to the reference DRGH antenna without a lens.

the E- and H-plane phase centers, and Figure 8 shows the axial symmetric dielectric lens on the DRGH antenna. The boresight directivities of the DRGH antenna with three different lenses, using the E-plane 1st quartile, 3rd quartile, and mode as focal points, are compared, in Figure 9, to the reference antenna (without a lens). The boresight directivities of the DRGH antenna with three lenses designed using the H-plane phase centers are shown in Figure 10. The boresight directivity of the DRGH antenna is remarkably insensitive to the three sets of focal points used for the lens design, over the whole frequency range from 1 to 18 GHz. All three lenses significantly increase the boresight directivity compared to the DRGH without a lens, and it was decided to use the phase center corresponding to the mode of the dataset when designing the bi-cylindrical lens.

The bi-cylindrical lens was realized by first designing an E-plane cylindrical lens with a hyperbolic profile. The dimension D_E is chosen to maximize the thickness of the E-plane cylindrical lens, which still fits inside the aperture of

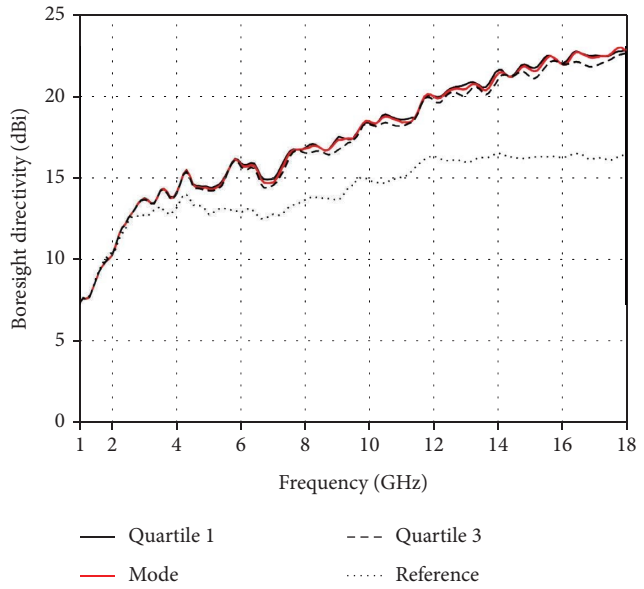

Figure 10: Boresight directivities of the DRGH antenna with an axial symmetric lens and three different H-plane focal distances, compared to the reference DRGH antenna without a lens.

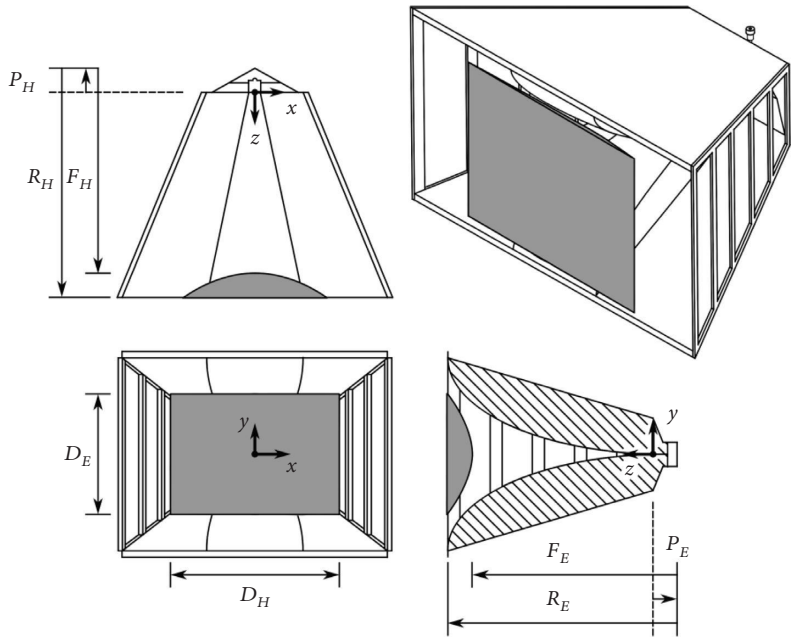

Figure 11: The DRGH antenna with a bi-cylindrical dielectric lens used to investigate the effect of different lens designs on the directivity performance of the antenna.

Table 3: Dimensions of the bi-cylindrical lens.

Symbol	Value (mm)	Description
P_E	−61.29	E-plane phase center offset from origin
P_H	3.17	H-plane phase center offset from origin
R_E	107.51	E-plane distance from the phase center to the aperture
R_H	171.97	H-plane distance from the phase center to the aperture
F_E	82.89	E-plane focal length
F_H	147.35	H-plane focal length
D_E	100	E-plane lens dimension
D_H	125.3	H-plane lens dimension

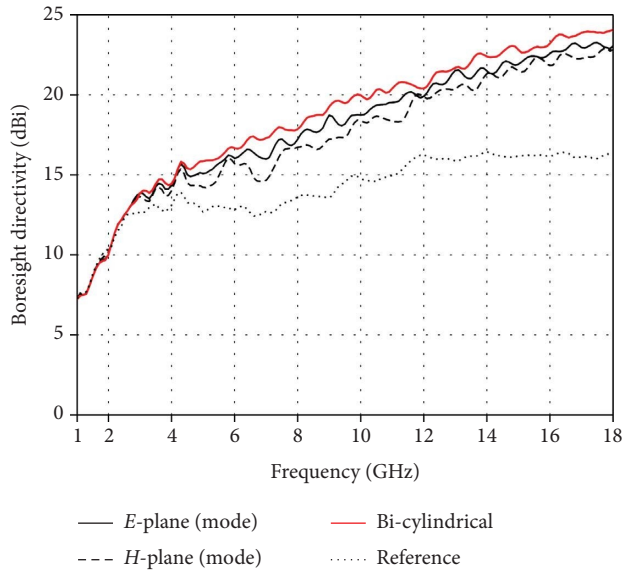

Figure 12: Boresight directivities of the DRGH antenna with three different lenses, E- and H-plane axial symmetric lenses and a bi-cylindrical lens.

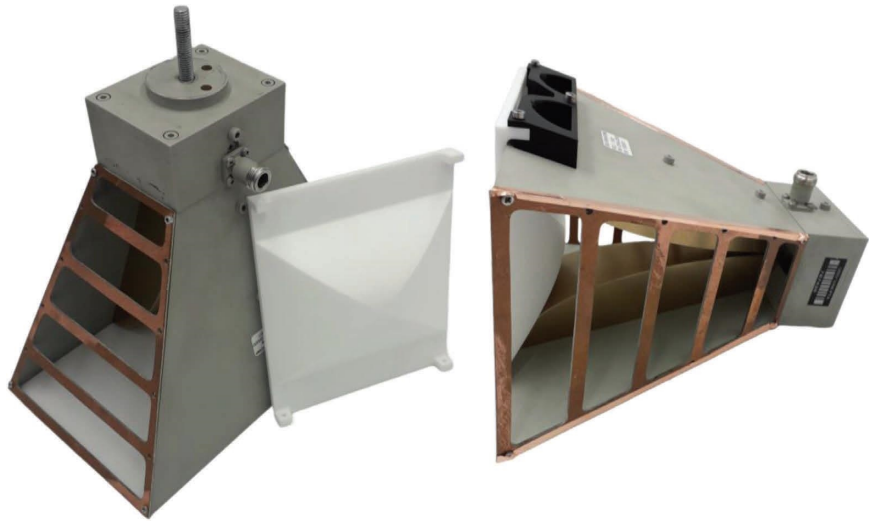

Figure 13: The DRGH antenna with a bi-cylindrical dielectric lens.

Table 4: Dimensions of the realized bi-cylindrical lens.

Symbol	Value (mm)	Description
P_E	−61.29	E-plane phase center offset from origin
P_H	3.17	H-plane phase center offset from origin
R_E	107.51	E-plane distance from the phase center to the aperture
R_H	171.97	H-plane distance from the phase center to the aperture
F_E	78.01	E-plane focal length
F_H	142.47	H-plane focal length
D_E	110	E-plane lens dimension
D_H	137.6	H-plane lens dimension

the DRGH. Subsequently, the H-plane cylindrical lens profile is obtained using the same lens thickness. This results in a lens with two different foci and diameters but the same thickness. Figure 11 shows the bi-cylindrical dielectric lens on the DRGH antenna, and the dimensions for the bi-cylindrical dielectric lens are given in Table 3. Figure 12 compares the directivity of the bi-cylindrical lens to that of the axial symmetric lenses designed with the E- and H-plane

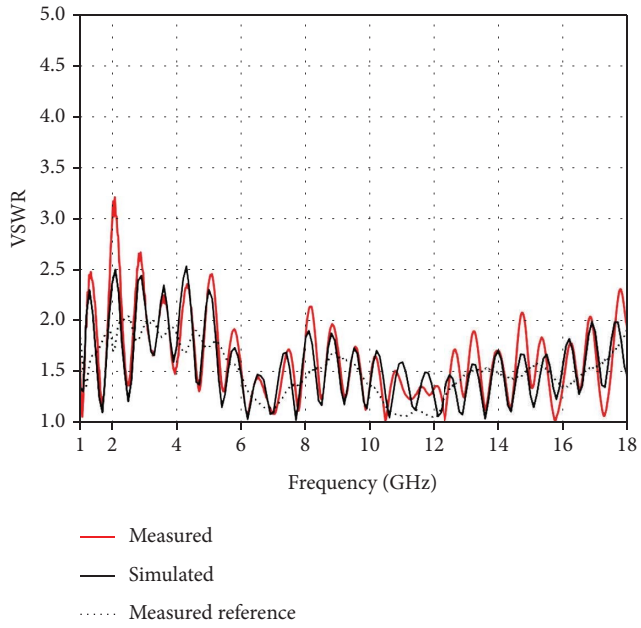

Figure 14: Simulated and measured VSWR of the DRGH antenna with and without the bi-cylindrical lens.

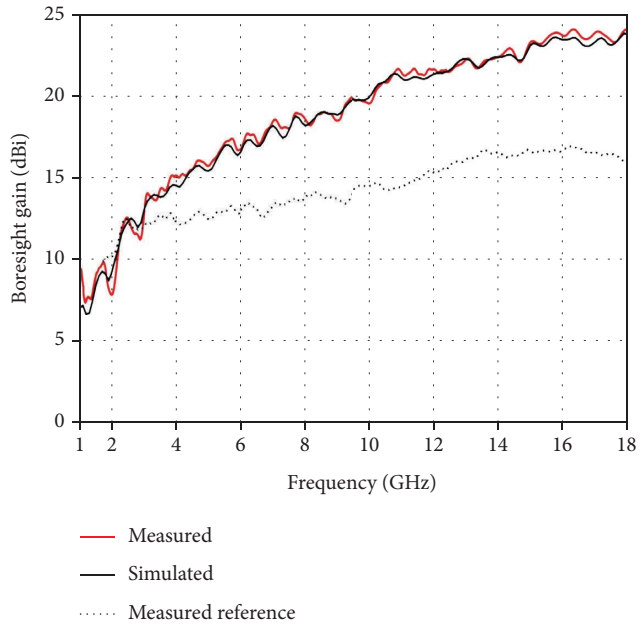

Figure 15: Simulated and measured boresight gain of the DRGH antenna with and without the bi-cylindrical lens.

phase centers, respectively. The E-plane axial symmetric lens outperforms the H-plane lens, with the bi-cylindrical lens outperforming both the E- and H-plane axial symmetric lenses.

3. Simulated and Measured Results

The realized bi-cylindrical lens is shown in Figure 13 and was designed using the modes as focal points and machined from a sheet of Virgin PTFE, KEYLON PTFE (PV1000), with a dielectric permittivity of 2.1 at 1 MHz. The dimensions are summarized in Table 4. It is small and compact, fits within the antenna aperture, only slightly increases the size of the DRGH, and is easily manufacturable.

The simulated and measured VSWR results are compared to the measured VSWR of the reference antenna in Figure 14. As expected, the addition of the lens slightly degraded the VSWR performance. Except for two regions between 2 and 3 GHz, the VSWR for the entire frequency range is below 2.5:1. Figure 15 shows the simulated and measured boresight gain of the DRGH antenna with and without the bi-cylindrical lens, measured in a compact

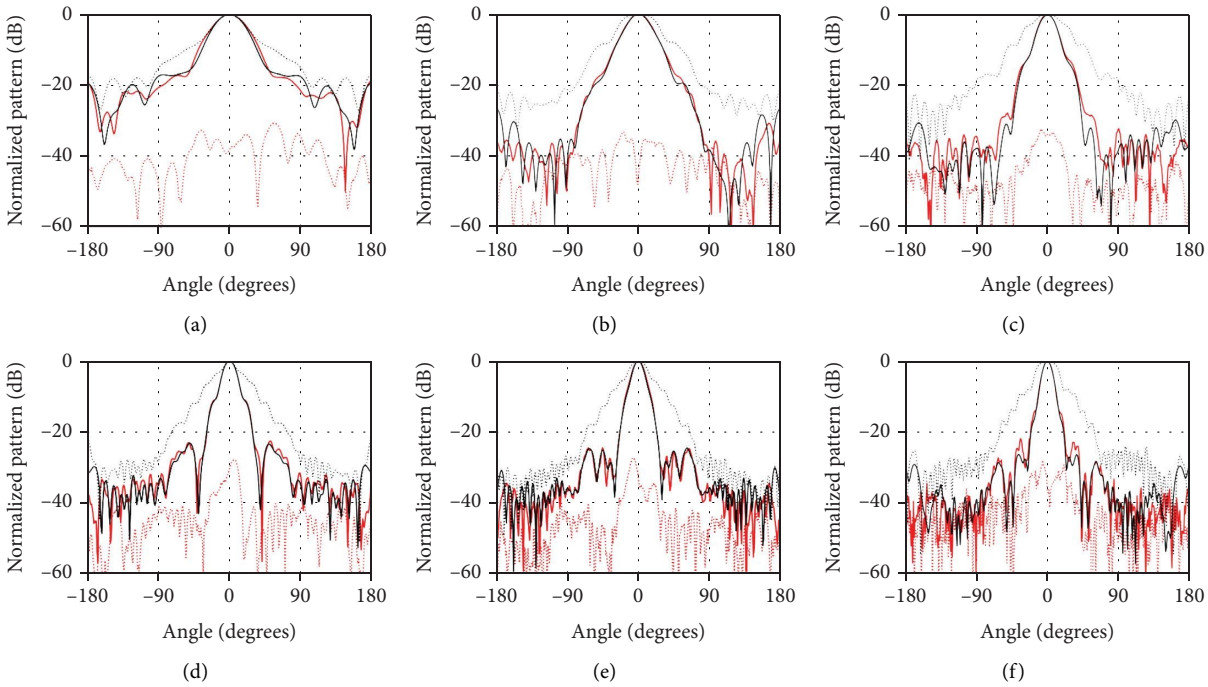

Figure 16: Simulated and measured E-plane radiation patterns of the DRGH antenna with and without the bi-cylindrical lens at (a) 3 GHz, (b) 6 GHz, (c) 9 GHz, (d) 12 GHz, (e) 15 GHz, and (f) 18 GHz (measured, measured X-pol, simulated, and reference).

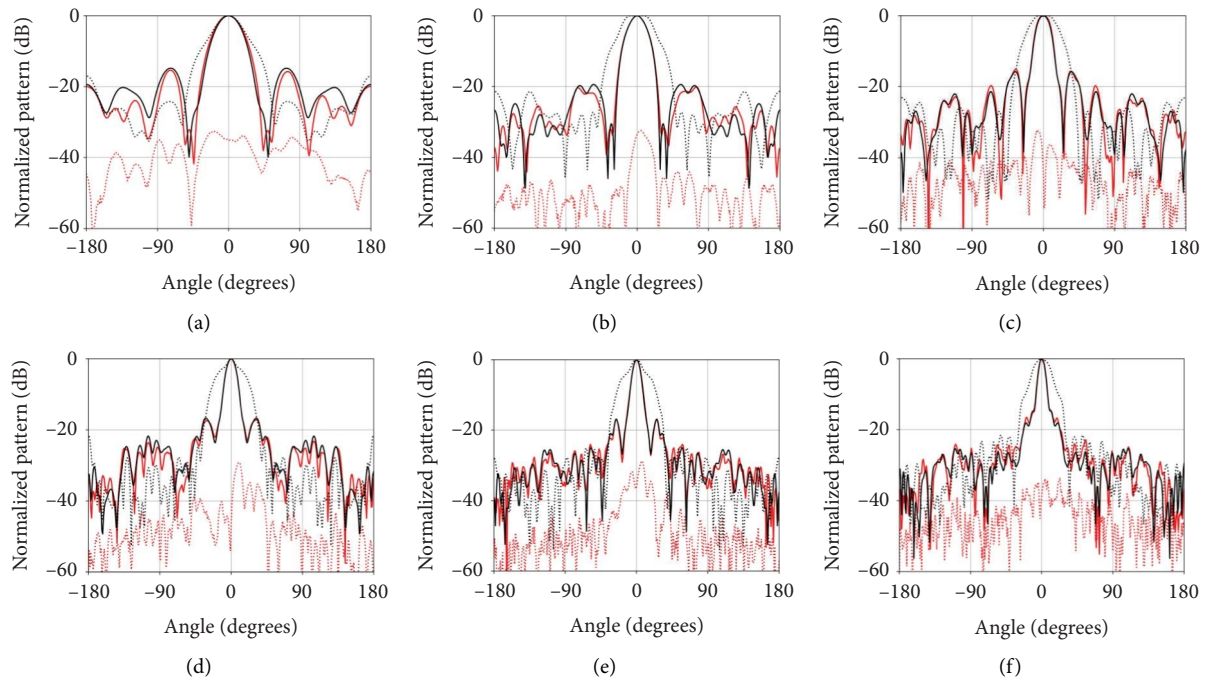

Figure 17: Simulated and measured H-plane radiation patterns of the DRGH antenna with and without the bi-cylindrical lens at (a) 3 GHz, (b) 6 GHz, (c) 9 GHz, (d) 12 GHz, (e) 15 GHz, and (f) 18 GHz (measured, measured X-pol, simulated, and reference).

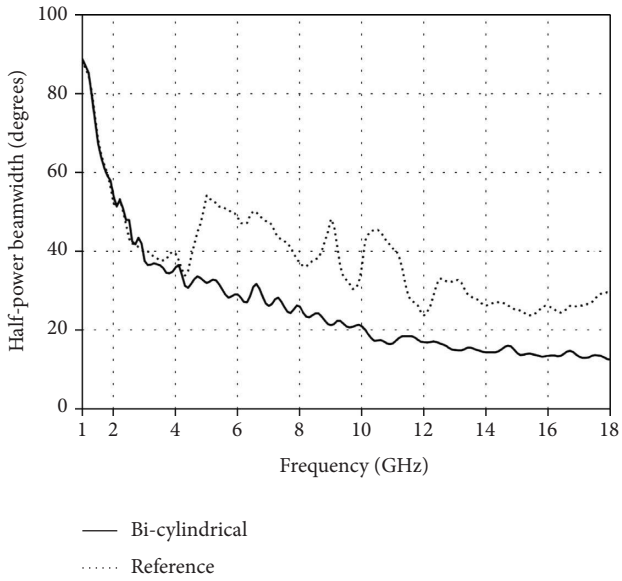

Figure 18: The simulated 3 dB beamwidth in the *E*-plane of the DRGH antenna with and without the bi-cylindrical lens.

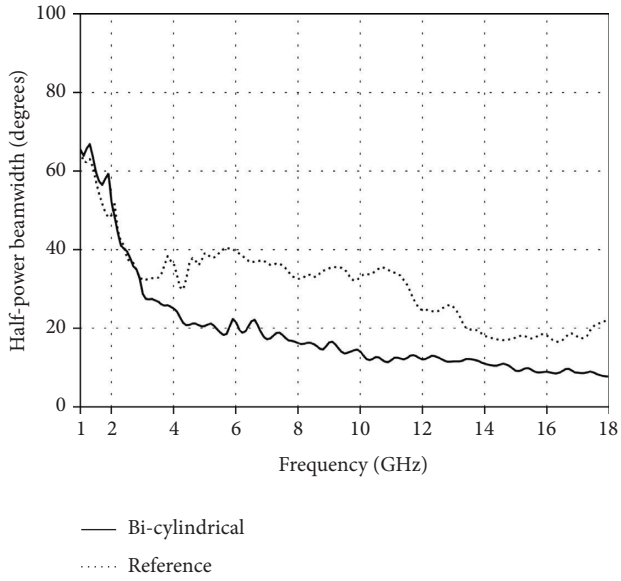

Figure 19: The simulated 3 dB beamwidth in the *H*-plane of the DRGH antenna with and without the bi-cylindrical lens.

Table 5: Comparison between the proposed antenna and previous research.

Ref.	Horn size with lens (mm^3)	Lens size (mm^3)	Bandwidth (GHz)	Gain (dBi)	Increase in gain (dB)
[15]	$242 \times 138.4 \times 209.8$	—	1–18	7–16.9	—
[8]	$244 \times 159 \times 200$	$100 \times 100 \times 30$	1–15	5–20	5
[9]	$61 \times 60 \times 161.69$	$84.86 \times 84.86 \times 77.1$	20–40	20.3–22	6
[10]	$50 \times 50 \times 86$	$50 \times 50 \times 8.7$	2–40	5–20.5	5
[11]	$488.4 \times 313.7 \times > 585$	$165 \times 360 \times 185$	0.4–6	12–18	5
[13]	$242 \times 136 \times 189$	$96.5 \times 96.5 \times 11$	1–18	7.2–19.5	4.5
This work	$242 \times 138.4 \times 209.8$	$137.6 \times 110 \times 29.5$	1–18	7–24.1	7

antenna test range. The lens significantly increases the boresight gain over the entire bandwidth, from a maximum of 16.9 dBi at 16 GHz to a maximum of 24.1 dBi at 18 GHz.

Figures 16 and 17 show the simulated and measured radiation patterns of the DRGH antenna with and without the bi-cylindrical lens for the *E*- and *H*-plane, respectively. The simulated and measured results are very similar , with the stable radiation patterns and well-defined main beams for all frequencies. As expected, the beamwidths for both the *E*- and *H*-plane patterns are reduced by the lens. Higher first sidelobe levels for the *H*-plane patterns are due to the straight vertical edges of the lens, while all the sidelobe levels for the *E*-plane patterns are significantly lower. Figures 18 and 19 show the 3 dB beamwidth in the *E*- and *H*-plane of the DRGH, respectively. The beamwidth varies less than $\pm 5^{\circ}$ over the frequency range from 4 to 18 GHz in both the *E*- and *H*-plane of the DRGH, compared to the $\pm 10^{\circ}$ for the DRGH without a lens.

Table 5 compares the performance of adding the proposed bi-cylindrical lens to the modified DRGH antenna from [15], with previous related research that implemented dielectric lenses on similar DRGH antennas. The bi-cylindrical lens significantly increases the boresight gain of the DRGH antenna without increasing the size of the modified DRGH [15]. The newly proposed DRGH with bi-cylindrical lens presented in this work increases the maximum gain by 7 dB compared to 4.5 dB for the very similar antenna presented in [13]. The proposed antenna is also significantly smaller with a larger increase in gain than the antennas operating in the same frequency range [8, 11]. The only antenna with approximately the same increase in gain is [9]. This antenna uses an external lens that significantly increases the length of the antenna from 74.9 mm to 161.69 mm, e.g., the length increases by more than 5.7 wavelengths at the lowest operating frequency.

4. Conclusion

A comprehensive wideband near-field *E*- and *H*-plane phase center analysis was performed for every wavefront at observation points over a region inside the flared section and outside the aperture of the DRGH. A plano-convex intersecting bi-cylindrical lens was designed using the two discrete phase centers corresponding to the statistical mode of the simulated phase distributions. The lens was implemented by intersecting two cylindrical dielectric lenses with hyperbolic profiles. This lens is a practical implementation of the bi-cylindrical lens, with both convex surfaces inside and a planar surface outside the DRGH. This makes manufacturing and mounting the lens much easier due to the planar surface providing the interface for adding dielectric mounting brackets, without significantly increasing the size of the DRGH antenna.

The bi-cylindrical lens significantly increases the boresight gain of the DRGH antenna, while simultaneously reducing the variation in 3 dB beamwidth over most of the operating band. Thus, adding the wideband lens to the modified DRGH antenna results in the desired properties of achieving a higher field strength and improving the field uniformity for antenna measurements and EMC/EMI testing.

Data Availability Statement

The data that support the findings of this study are available from the corresponding author upon reasonable request.

Conflicts of Interest

The authors declare no conflicts of interest.

Funding

No funding was received for this study.

Acknowledgments

The authors are grateful for the support received from Saab Grintek Defence for the manufacturing of the bi-cylindrical lens and the use of their anechoic chambers and production facilities.

References

[1] "Requirements for the Control of Electromagnetic Interference Characteristics of Subsystems and Equipment, Standard MIL-STD-461G" (2015).

[2] C. Bruns, P. Leuchtmann, and R. Vahldieck, "Analysis and Simulation of a 1–18 GHz Broadband Double-Ridged Horn Antenna," *IEEE Transactions on Electromagnetic Compatibility* 45, no. 1 (2003): 55–60.

[3] B. Jacobs, J. W. Odendaal, and J. Joubert, "An Improved Design for a 1–18 GHz Double-Ridged Guide Horn Antenna," *IEEE Transactions on Antennas and Propagation* 60, no. 9 (2012): 4110–4118, https://doi.org/10.1109/tap.2012.2207043.

[4] M. Abbas-Azimi, F. Arazm, and J. Rashed-Mohassel, "Sensitivity Analysis of a 1 to 18 GHz Broadband DRGH Antenna," in *2006 IEEE Antennas and Propagation Society International Symposium* (Albuquerque, NM, May 2006).

[5] B. Jacobs, J. W. Odendaal, and J. Joubert, "The Effect of Manufacturing and Assembling Tolerances on the Performance of Double-Ridged Horn Antennas," *Journal of Electromagnetic Waves and Applications* 24, no. 10 (2010): 1279–1290, https://doi.org/10.1163/156939310791958761.

[6] V. Rodriguez, *New Broadband EMC double-ridge Guide Horn Antenna* (RF Design, 2004).

[7] B. Jacobs, J. W. Odendaal, and J. Joubert, "Compact 0.5–18 GHz Double-Ridged Guide Horn Antenna," *IET Microwaves, Antennas & Propagation* 15, no. 4 (2021): 427–440, https://doi.org/10.1049/mia2.12058.

[8] A. S. Turk and A. K. Keskin, "Partially Dielectric-Loaded Ridged Horn Antenna Design for Ultrawideband Gain and Radiation Performance Enhancement," *IEEE Antennas and Wireless Propagation Letters* 11 (2012): 921–924, https://doi.org/10.1109/lawp.2012.2211071.

[9] S. Demirel, A. Caliskan, and M. T. Mersin, "Design of Dielectric Lens Loaded Double Ridged Horn Antenna for Millimetre Wave Application," in *2016 21st International Conference on Microwave, Radar and Wireless Communications (MIKON)* (Krakow, Poland, May 2016).

[10] Tenigeer, N. Zhang, J. Qiu, P. Zhang, and Y. Zhang, "Design of a Novel Broadband EMC Double Ridged Guide Horn Antenna," *Progress in Electromagnetics Research C* 39 (2013): 225–236, https://doi.org/10.2528/pierc13032803.

[11] A. Mehdipour, Z. Chen, and L. Matytsine, "Customized Compact Dielectric Lens to Improve Double-Ridge Horn Antenna Performance for Automotive Immunity EMC Test," in *2016 IEEE International Symposium on Electromagnetic Compatibility (EMC)* (Ottawa, Canada, July 2016).

[12] P. D. Kuroptev, V. V. Levyakov, and A. V. Fateev, "Modified 0.6–50 GHz Ultra-Wideband Double-Ridged Horn Antenna Design for Parameters Improvement," in *2017 47th European Microwave Conference (EuMC)* (Nuremberg, Germany, October 2017).

[13] Y. Zhang, D. Wang, L. Deng, L. Zhang, X. Yuan, and Y. Long, "Broadband Dielectric-Loaded Horn Antenna With Enhanced Gain for 1–18 GHz EMC Applications," in *2022 IEEE 5th International Conference on Electronics Technology (ICET)* (Chengdu, China, May 2022).

[14] K. L. Walton and V. C. Sundberg, "Broadband Ridged Horn Design," *Microwave Journal* 11 (1964): 96–101.

[15] M. Gerber, J. W. Odendaal, and J. Joubert, "DRGH Antenna With Improved Gain and Beamwidth Performance," *IEEE Transactions on Antennas and Propagation* 68, no. 5 (2020): 4060–4065, https://doi.org/10.1109/tap.2019.2948655.

[16] Dassault Systèmes, "CST Studio Suite Electromagnetic Field Simulation Software," (2024), https://www.3ds.com/products/simulia/cst-studio-suite.